MULTIPLE-FACTOR ANALYSIS OF LOWER IONOSPHERIC PERTURBATIONS BASED ON VLF OBSERVATIONS

VIKTOR FEDUN, SERGEY RUZHEINIKOV

MARIYA SOLOVIEVA AND ALEXANDER ROZHNOI

Space Systems Laboratory,
Automatic Control and Systems Engineering,
The University of Sheffield,
v.fedun@sheffield.ac.uk

Institute of Physics of the Earth,
Russian Academy of Sciences, Moscow, Russia
rozhnoi@ifz.ru

EARTH'S IONOSPHERE

- The charged part of the atmosphere (partially ionized gas);
- Solar UV and X-ray radiation dominates the ionization processes during the day;
- During the night, non-solar sources (e.g., cosmic rays, meteoric ionization, etc.) maintain the smaller free electrons and ions concentrations;
- The ionosphere is divided into four main regions: D, E, F1, and F2 regions. Each of the regions is characterized by its ion's composition and concentration, as well as its own physics.

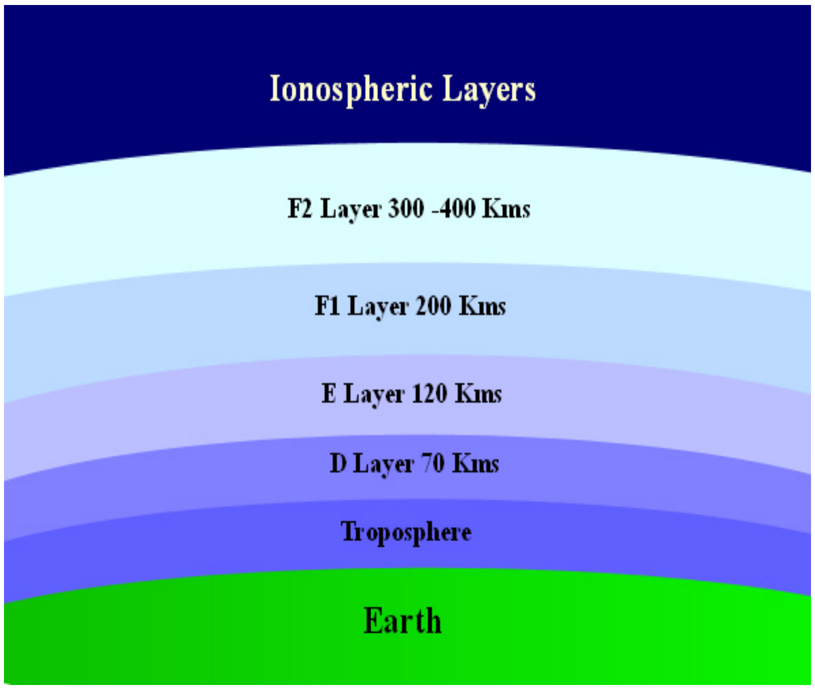

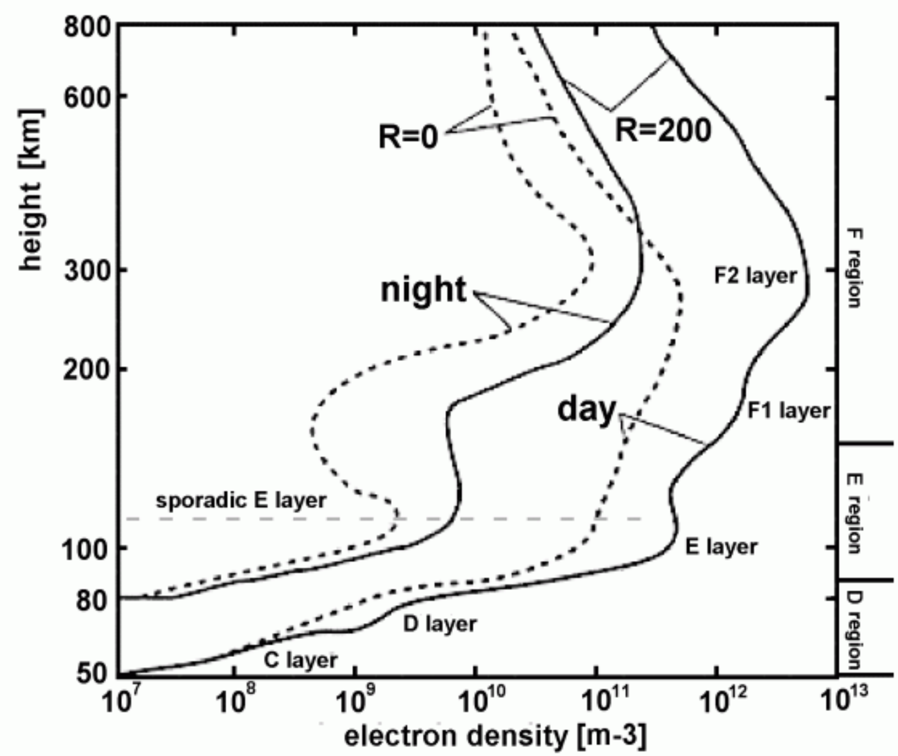

VERY LOW FREQUENCY (VLF)

Very Low Frequency (VLF, 3-30 kHz) EM signals from navigational or time service transmitters propagate inside the earth-ionosphere waveguide and they are reflected by the D region, at an altitude of ~65 km during daytime, and ~85 km during nighttime. The received signals inherently contain information of the reflection height's region and its variability.

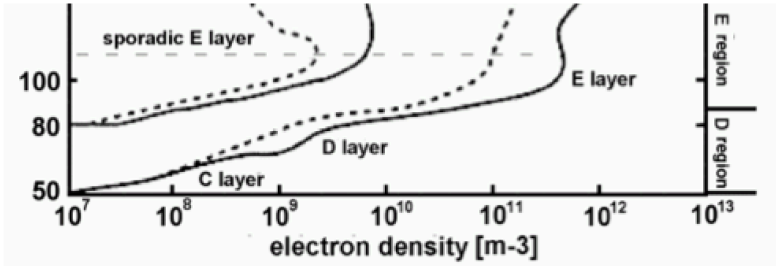

Therefore, VLF measurements allow studying the ionosphere in the D region. This is a great advantage, as these heights are too high to study them by using balloons, and too low for in-situ measurements of satellites. Moreover, measurements with the use of rockets, are very transient and spatially limited.

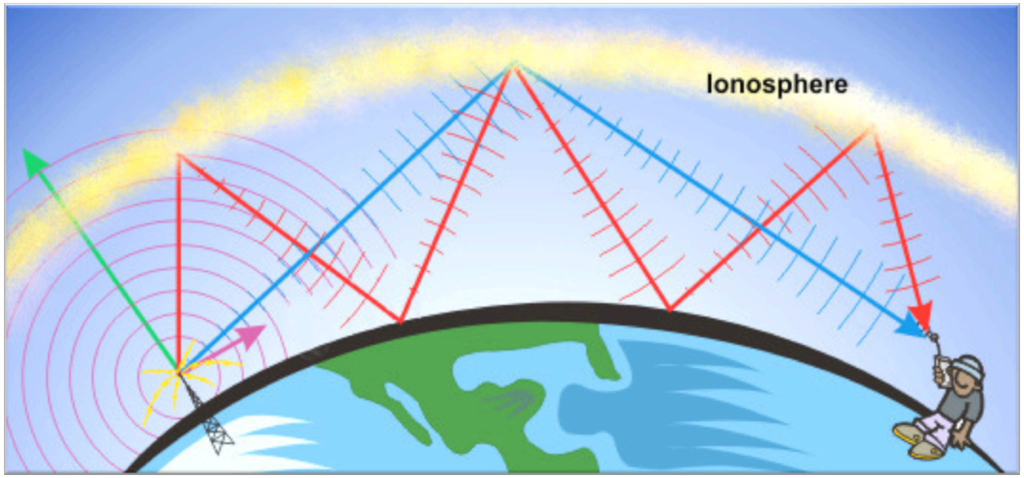

OUR CURRENT NETWORK OF VLF RECEIVERS

2010 P.-Kamchatsky (158.92 E 53.15N)
2010 Sakhalin Yuzhno-Sakhalinsk (142.75 E 46.96N)
2010 Moscow (37.7 E 55.75 N)
2011 Yuzhno-Kurilsk (145.861E 44.035N)
2010 Graz (15.431 E 47.065 N)
2013 Kirgizia (74.41 E 42.40 N)
2013 Sheffield (1’28.67” WE 53.22.89”)
2015 Varanasi (82.99 E 25.259 N)
2010 Japan
2015 LA, USA
2016 Birr, Ireland
2016 Tel Aviv, Israel

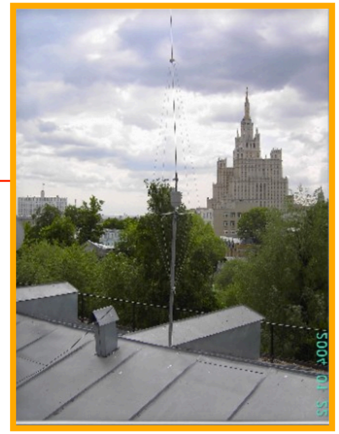

DHO 23.4 kHz
TBB 26.7 kHz
NRK 37.5 kHz
ITS 45.9 kHz
GBS 19.58 kHz
NAA 24.0 kHz
ICV 20.27 kHz
NPM 21.4 kHz

DHO 23.4 kHz
TBB 26.7 kHz
NAA 24.0 kHz
ICV 20.27 kHz
NPM 21.4 kHz
ITS 45.9 kHz
NWC 19.8 kHz
NLK 24.8 kHz
NRK 37.5 kHz
GBS 19.58 kHz
FTA 20.9 kHz
GQD 22.1 kHz
HWU 18.2 kHz
NML 25.2 kHz

DHO 23.4 kHz
TBB 26.7 kHz
NRK 37.5 kHz
ITS 45.9 kHz
GBS 19.58 kHz
NAA 24.0 kHz
ICV 20.27 kHz
NPM 21.4 kHz

DHO 23.4 kHz
TBB 26.7 kHz
NAA 24.0 kHz
ICV 20.27 kHz
NPM 21.4 kHz
JJI 22.2 kHz
NWC 19.8 kHz
ICV 20.27 kHz
NAA 24.0 kHz
NTS 18.6 kHz
JJY 40.0 kHz
VTX 16.3 kHz
VTX 17.0 kHz
VTX 18.2 kHz
VTX 19.2 kHz

DHO 23.4 kHz
TBB 26.7 kHz
NAA 24.0 kHz
ICV 20.27 kHz
NPM 21.4 kHz
JJI 22.2 kHz
NWC 19.8 kHz
VTX 17.0 kHz

OUR CURRENT NETWORK OF VLF RECEIVERS

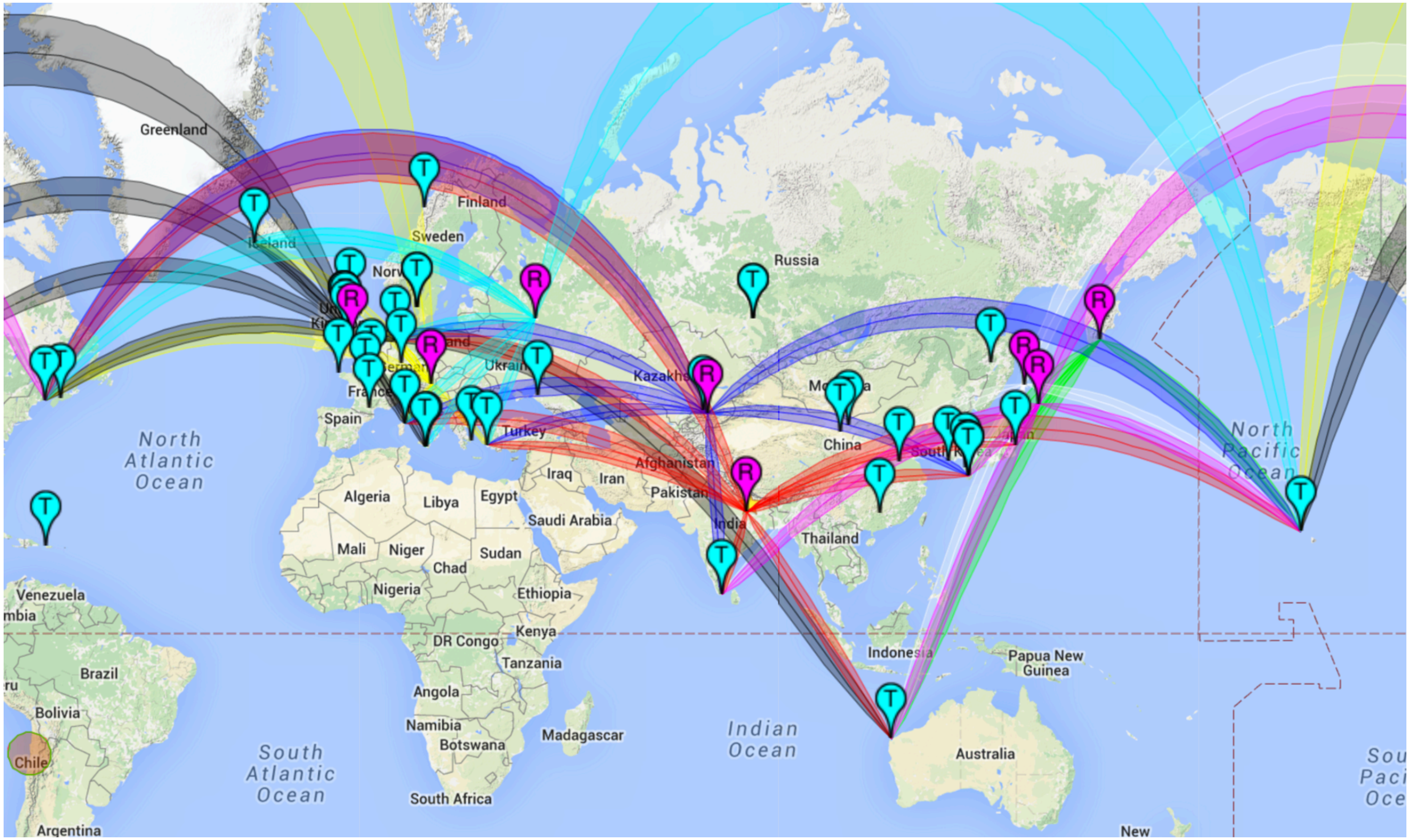

World Geodetic System (WGS) 1984

Radius of preparing earthquake

$$\rho = 10^{0.43\,M}\ \mathrm{km}$$

Dobrovolskiy, 1979

FRESNEL ZONE

The **Fresnel zone** is the zone of **VLF/LF** signal sensitivity to perturbations in the medium during propagation.

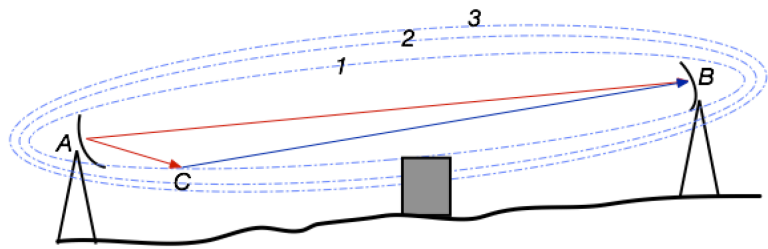

Fresnel zones are concentric ellipses (1, 2, 3) centred on the direct transmission path (AB). In these elliptical area the transmitter and receiver are in foci (*Wait, 1964*).

Radio waves travel in a straight line from the transmitter to the receiver. But if there are reflective surfaces along the path, such as bodies of water or smooth terrain, the radio waves reflecting off those surfaces may arrive either out of phase or in phase with the signals that travel directly to the receiver. Waves that reflect off of surfaces within an **even (2, ..)** Fresnel zone are out of phase with the direct-path wave and reduce the power of the received signal. Waves that reflect off of surfaces within an **odd** Fresnel zone (1, 3, 5) are in phase with the direct-path wave and can **enhance the power** of the received signal.

In general, we analysing the earthquakes with their epicenters inside three Fresnel zones (the sensitivity zone). Along the path the semi-width (*y*) of the 1st zone on the ground is approximated described by the formula:

$$y \approx \left[\frac{\lambda^2}{4} + \lambda x \left(l - \frac{x}{D}\right)\right]^{1/2}$$

were λ is wavelength, *D* – distance between the receiver and the transmitter and were *x* is the coordinate along the path *D*.

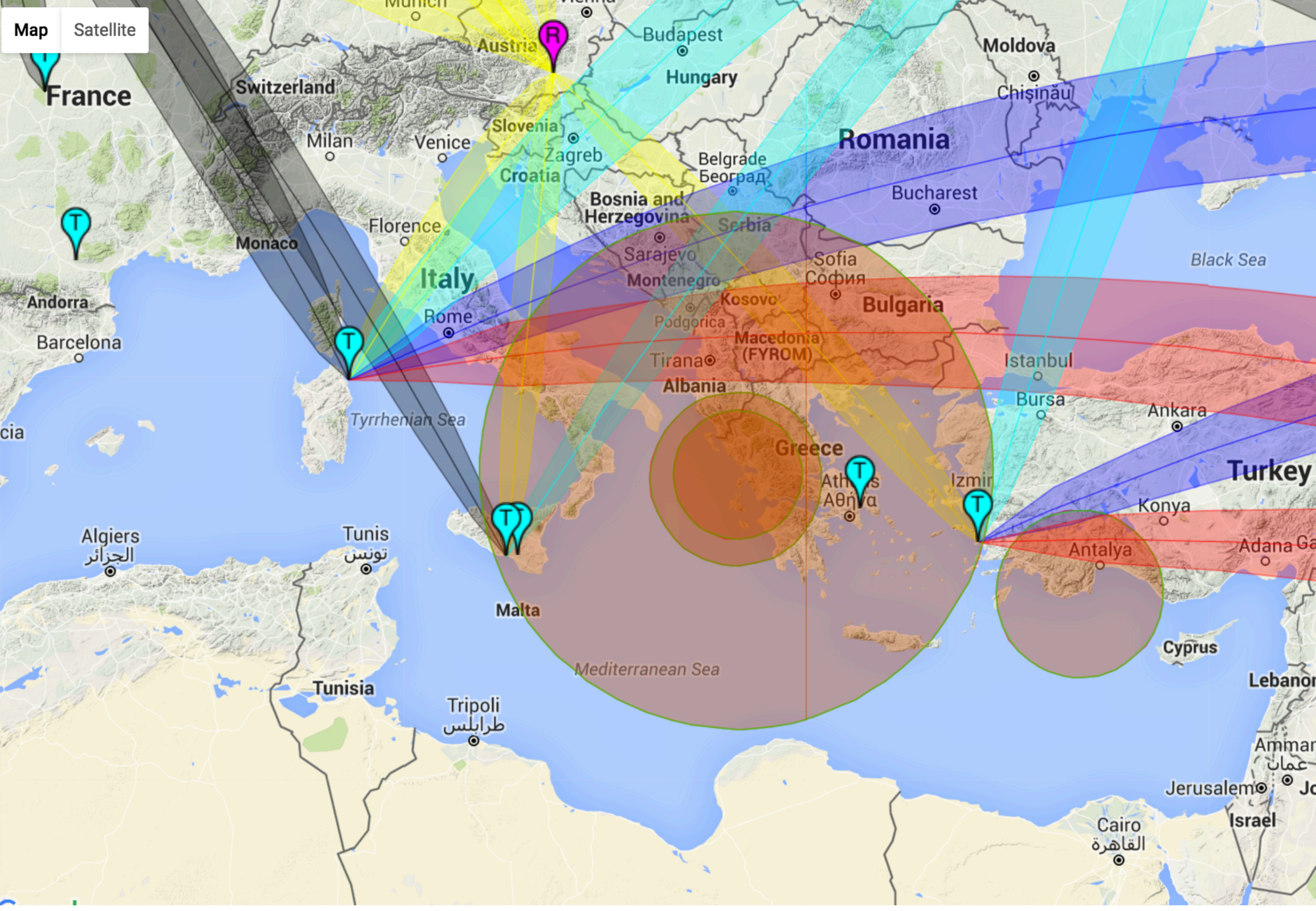
Map
Satellite
Munich
Vienna
Austria
Budapest
Hungary
Moldova
Chișinău
France
Switzerland
Slovenia
Milan
Venice
Zagreb
Croatia
Romania
Belgrade
Београд
Bucharest
Bosnia and Herzegovina
Serbia
Florence
Monaco
Sarajevo
Sofia
София
Black Sea
Montenegro
Italy
Kosovo
Bulgaria
Andorra
Rome
Podgorica
Barcelona
Macedonia (FYROM)
Tirana
Istanbul
Albania
Bursa
Ankara
Tyrrhenian Sea
Greece
Turkey
Athens
Αθήνα
Izmir
Konya
Algiers
الجزائر
Tunis
تونس
Antalya
Adana
Malta
Cyprus
Lebanon
Mediterranean Sea
Tunisia
Tripoli
طرابلس
Amman
عمان
Jerusalem
Israel
Cairo
القاهرة

THE MAIN AREAS OF THE WORK

1. Investigation of forcing from below (natural hazards events):

- Earthquakes
- Tsunamis
- Volcanic eruptions
- Extreme weather events – tropical cyclones (typhoons in the Pacific Ocean and hurricanes in the Atlantic Ocean)

2. Investigation of forcing from above:

- Magnetic storms (caused by interaction of the solar wind with the Earth's magnetosphere)
- Solar flare
- Electron out-zone fluxes and proton bursts

THE MAIN OBJECTIVES OF THE INVESTIGATIONS ARE

- Development of physical models of lithosphere-atmosphere-ionosphere coupling.
- Practical use of the obtained results for prediction and monitoring of natural hazards events.

X-RAYS INFLUENCE

Sudden phase anomalies (SPA) in VLF/LF signals in daytime are caused by X-rays emitted during solar flares. They are observed in 2-3 min after the radiation registration in satellite the GOES.

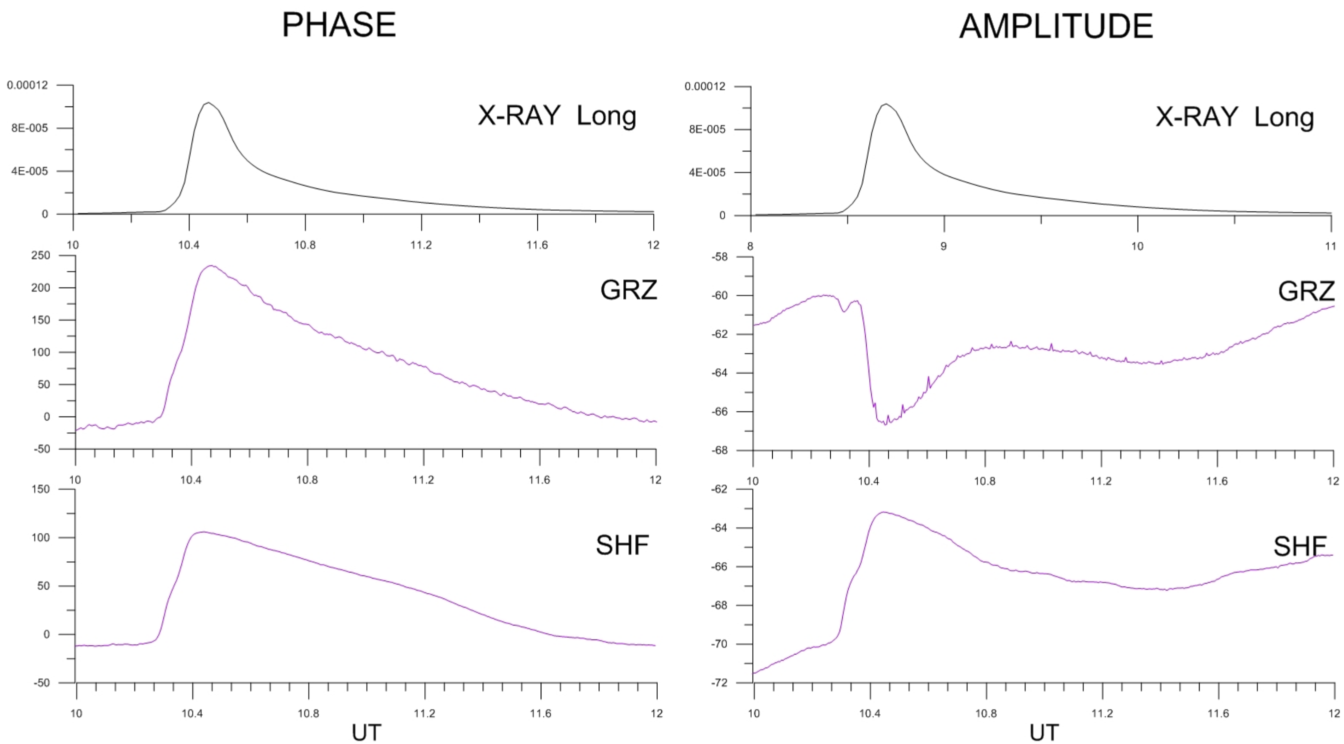

An example of SPAs in Iceland-Graz (Austria) and Iceland-Sheffield paths during the solar flare of intensity class X1.0 on November 19, 2013.

X-RAYS INFLUENCE

Ionospheric disturbances associated with a number of flares on 2 October 2015 using our Stanford SID at Birr Castle, Ireland.

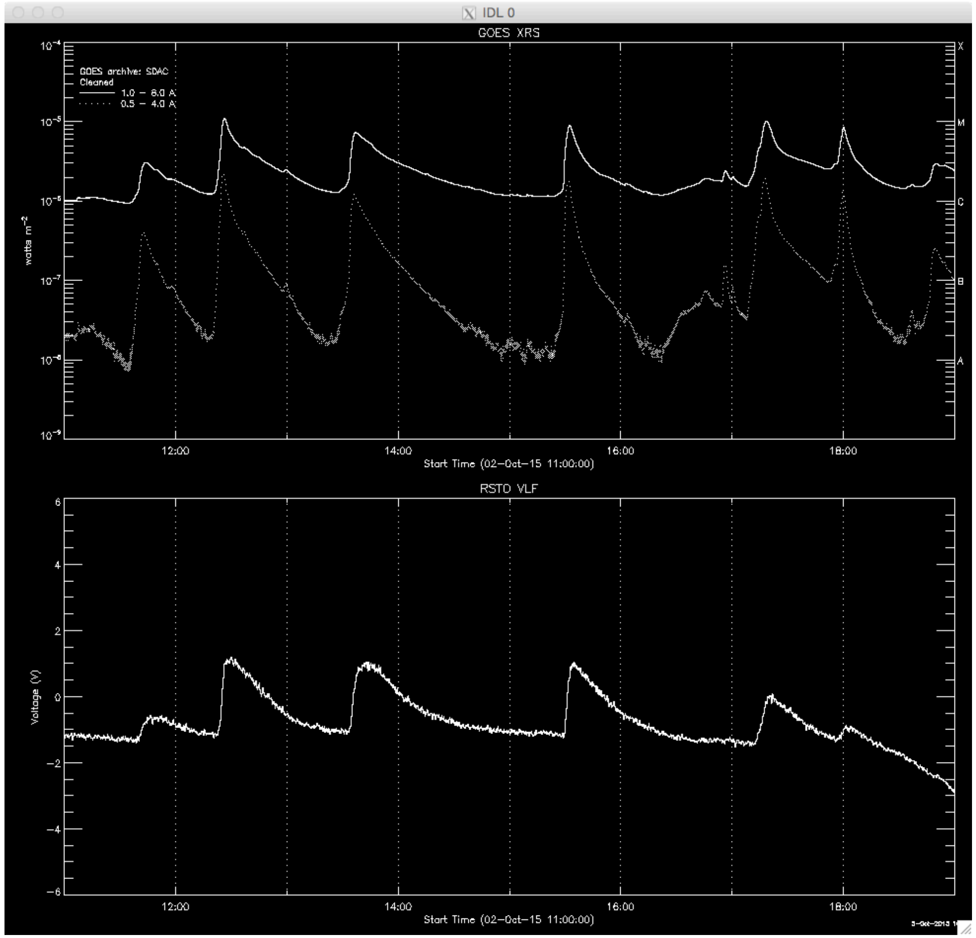

courtesy to Prof Peter Gallagher, TCD, Ireland
peter.gallagher@tcd.ie

EXAMPLE OF THE DAILY RESIDUAL SIGNAL dA(t) AND dP(t) DETERMINATION

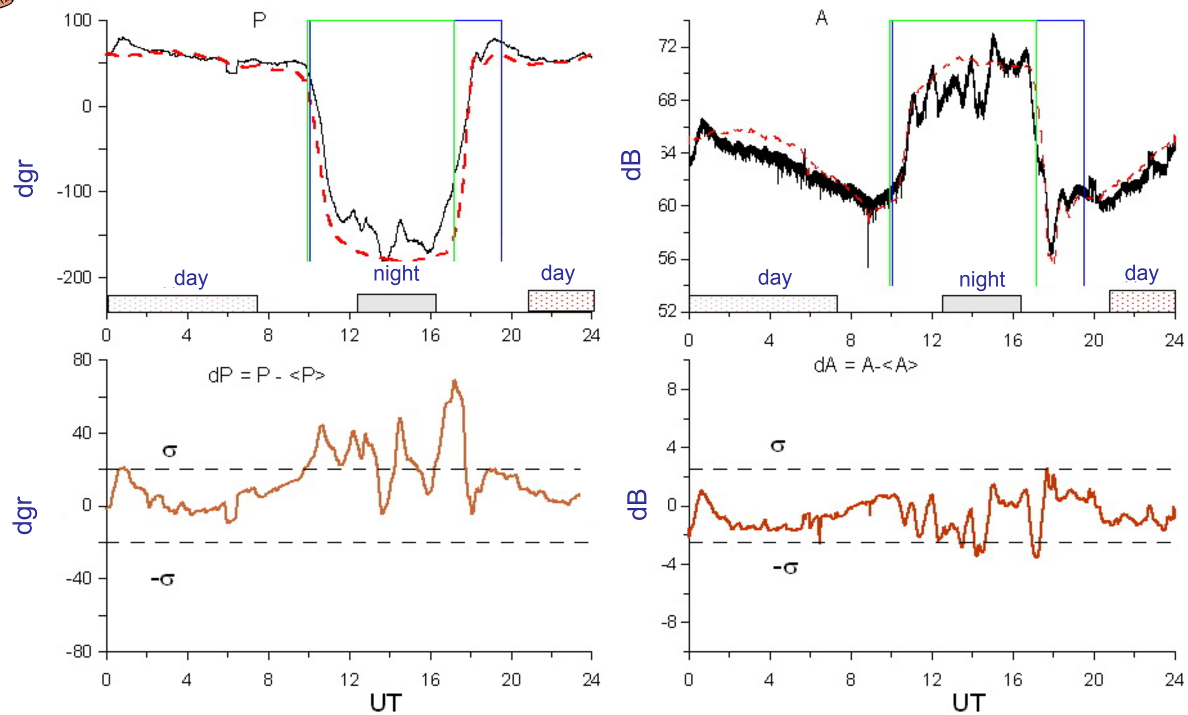

current values of phase (P) and amplitude (A) of the signal
monthly averaged values of <A> and <P>
lines of the sunrise and sunset in Japan
lines of the sunrise and sunset in P. Kamchatskiy

$$\mathrm{d}A(t) = A(t) - \langle A \rangle, \quad \mathrm{d}P(t) = P(t) - \langle P \rangle$$

Method of analysis

The **day** and **nighttime** ionosphere has different characteristics. Solar UV and X-ray radiation dominates the ionization processes during the day, so effect of ionization is significant. During night time, the non-solar sources (e.g. cosmic rays, meteoric ionization, etc.) maintain the less free electrons and ions concentrations.

Nighttime ionosphere is not very stable and provides optimal conditions for the detection of ionospheric disturbances by the VLF/LF signals.

Our data processed by analysing the difference between the real signal in nighttime and the model (*Rozhnoi et al., 2004*). The model for the ground-based observation is based on **monthly averaged signals** calculated by using data from **quiet days**. The models of the **seasonal variation** in the amplitude and phase of signals are used to remove the general trends in the data, leaving a residual signal of phase dP or amplitude dA which is defined as the difference between observed signal P(t), A(t) and model signal <P>, <A>:

MAGNETIC STORM INFLUENCE

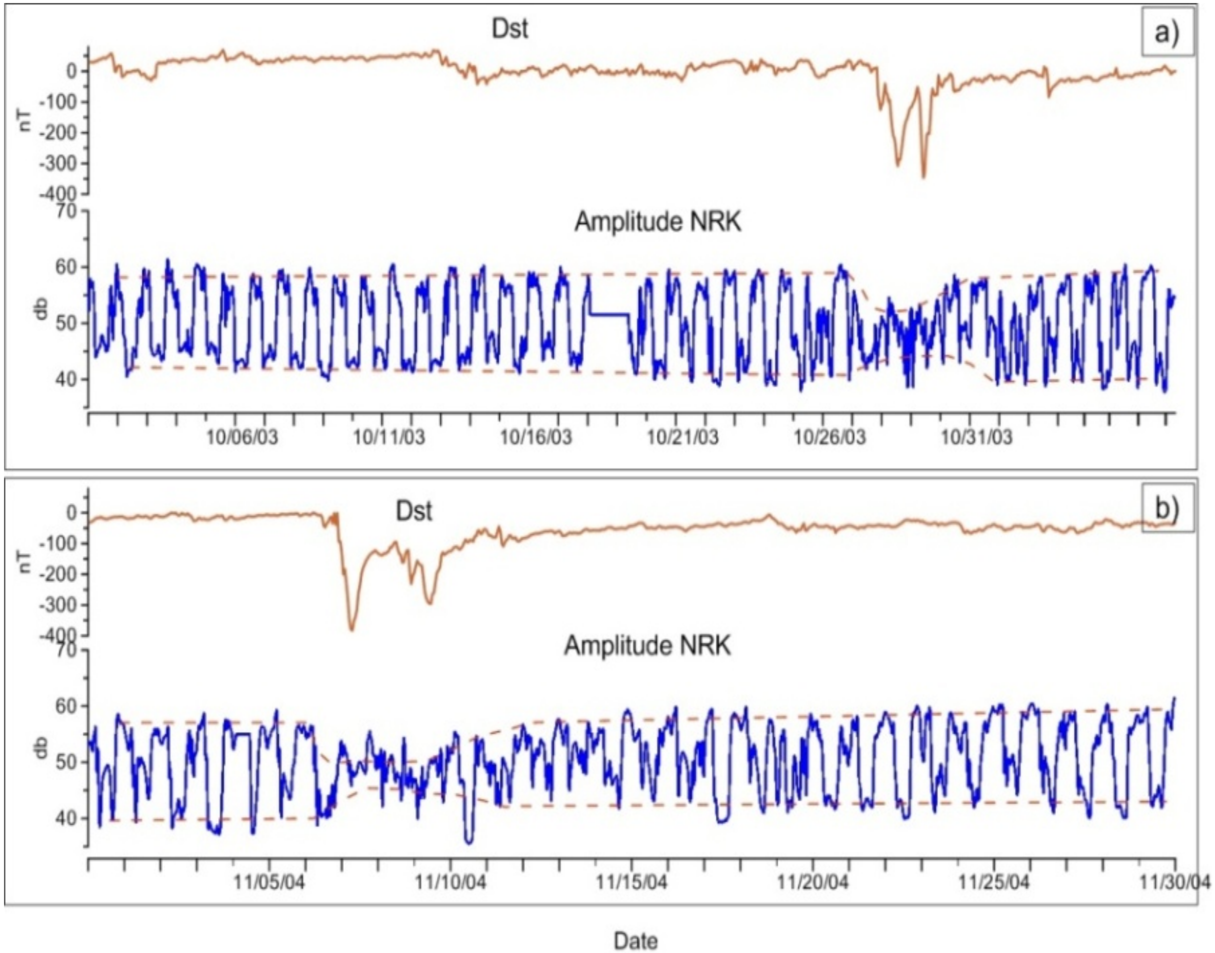

Variations of the amplitude of the LF signal (37.5 kHz) in the wave path NRK – Bari during periods of strong magnetic activity (Dst~-400 nT) in the path Iceland-Bari (Italy): a) magnetic storm in October 28-31, 2003; b) magnetic storm in November 8-10, 2004.

SEASONAL VARIATION

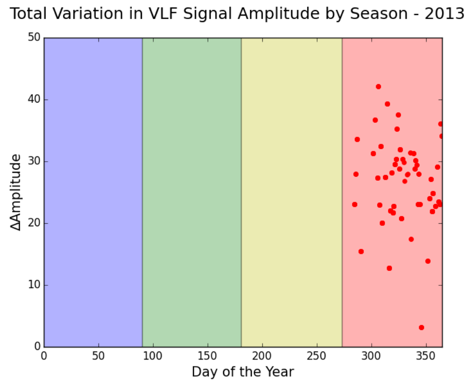

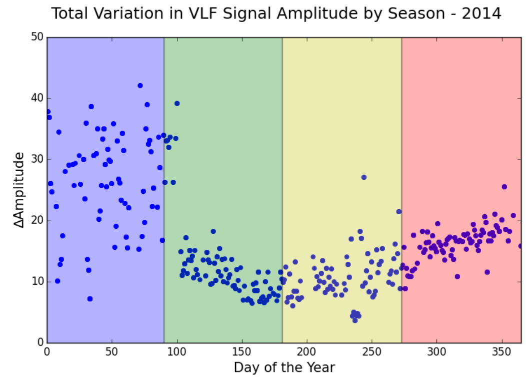

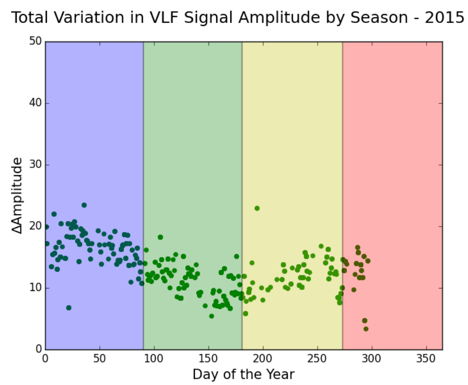

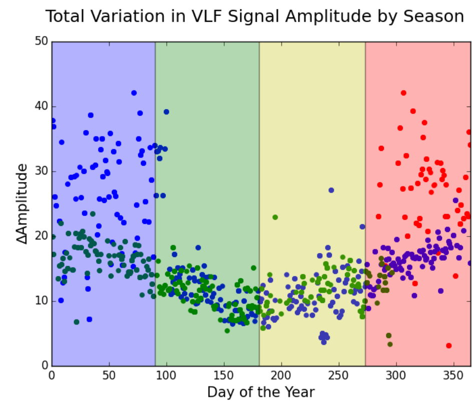

Winter - Jan -> Mar

Spring - Apr -> Jun

Summer - Jul ->Sep

Autumn - Oct -> Dec

courtesy to Dr Aengus Rae TCD, Ireland
raea@tcd.ie

Chrissan & Fraser-Smith, Radio Science, **31**, 5, Pages 1141-1152, 'September-October 1996 Seasonal variations of globally measured ELF/VLF radio noise'

Done: A global survey of extremely low frequency (ELF) and very low frequency (VLF) radio noise since February 1985

Found: The noise amplitudes vary seasonally by up to a factor of 4 in some of the sixteen frequency band.

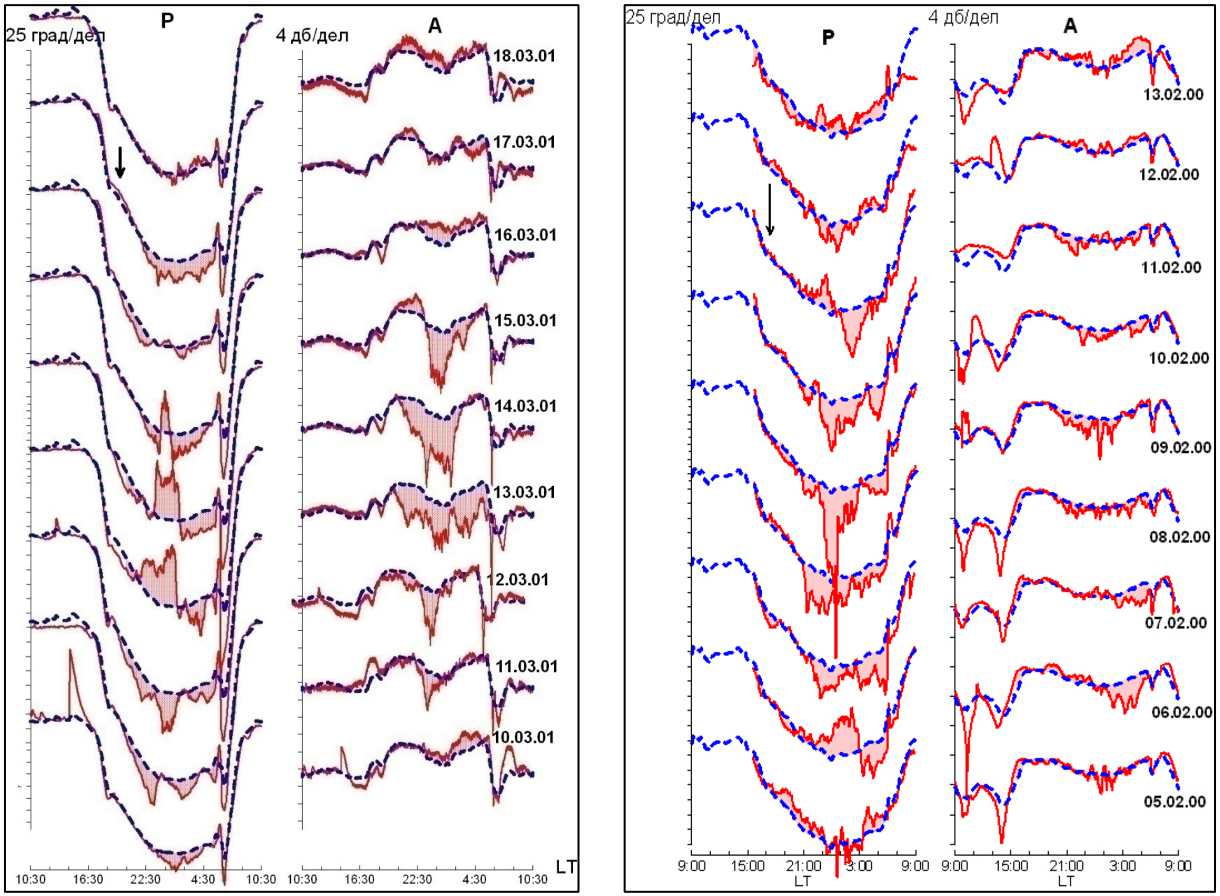

Phase and amplitude anomalous of the LF signal (40 kHz) before:

- Earthquake in P.-Kamchatsky on 17 March 2001, M=5.5, left;
- Moshiri before earthquake 11 February 2000, M=5.1

The arrows show the date of earthquake. Dash line shows the average level of signal for quiet days.

MAGNETIC STORM INFLUENCE

Magnetic storms with -150 <Dst< -100 nT don't influence considerably on characteristics of the VLF/LF signals. Analysis made for 24 midlatitudes paths in the Far East and European networks revealed amplitude anomalies during the main and recovery phases for several magnetic storms only for three the northernmost paths.

Correlation of the signals with magnetic activity is **rather weak** even for these paths (less than 20%).

For the majority of paths the correlation was not revealed.

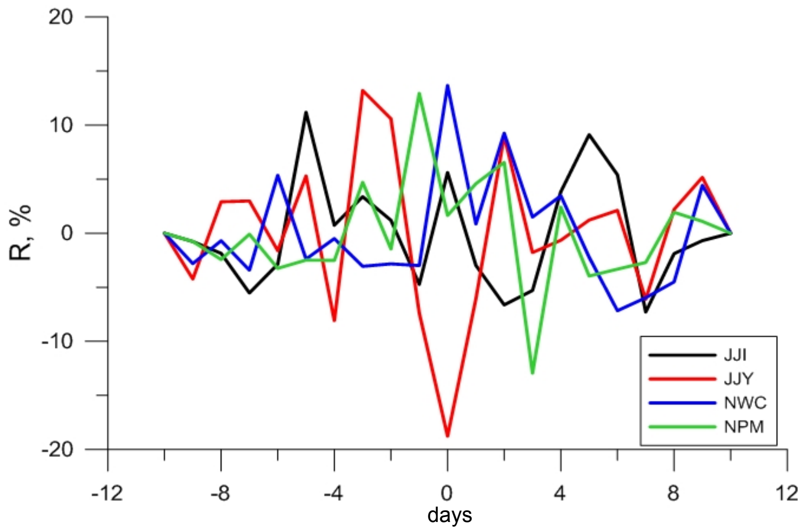

An example of the cross-covariance functions for the average residual amplitude in nighttime of the signals received in Petropavlovsk-Kamchatsky station and Max Dst indexes calculated in the interval ± 10 days for 2012. Axis Y is the correlation coefficient. Axis X is days.

INFLUENCE OF PROTON BURSTS AND RELATIVISTIC ELECTRON FLUXES

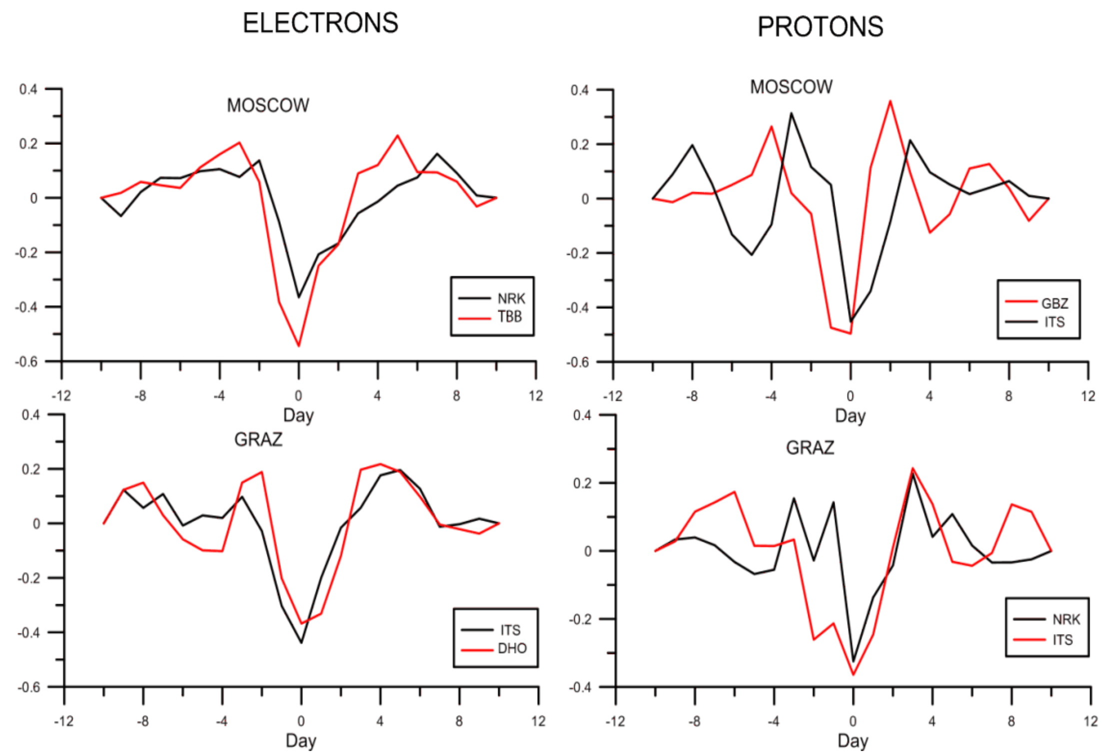

Examples of cross-covariance functions for the average residual amplitude in nighttime of several signals receiving in Moscow and Graz stations and the electron (left) and proton (right) fluxes (GOES the satellite). Axis Y is the correlation coefficient. Axis X is days. The influence is **rather significant** (~ 40 %).

EARTHQUAKE IN L'AQUILA (ITALY) M=6,3, 6 APRIL 2009

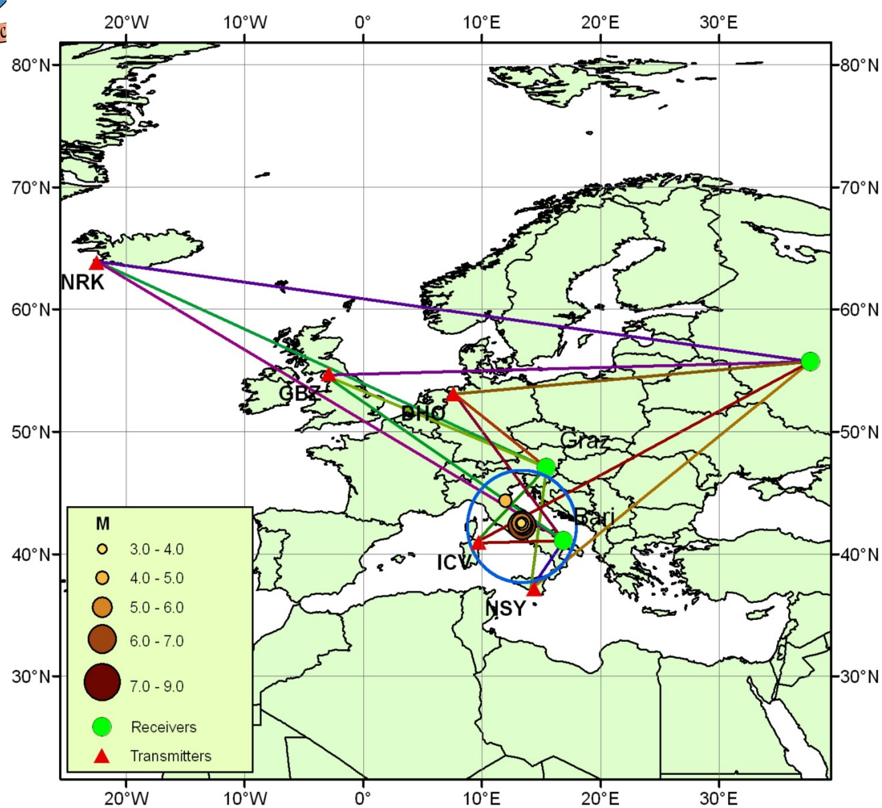

A map showing position of the transmitters and receivers in Moscow, Bari and Graz together with the epicenters of the earthquakes occurred in the Abruzzo area in the period April 1-9, 2009. The blue circle represents the projection on the ground surface of the perturbed zone in the atmosphere-ionosphere boundary that approximately coincides with a zone of precursory activity.

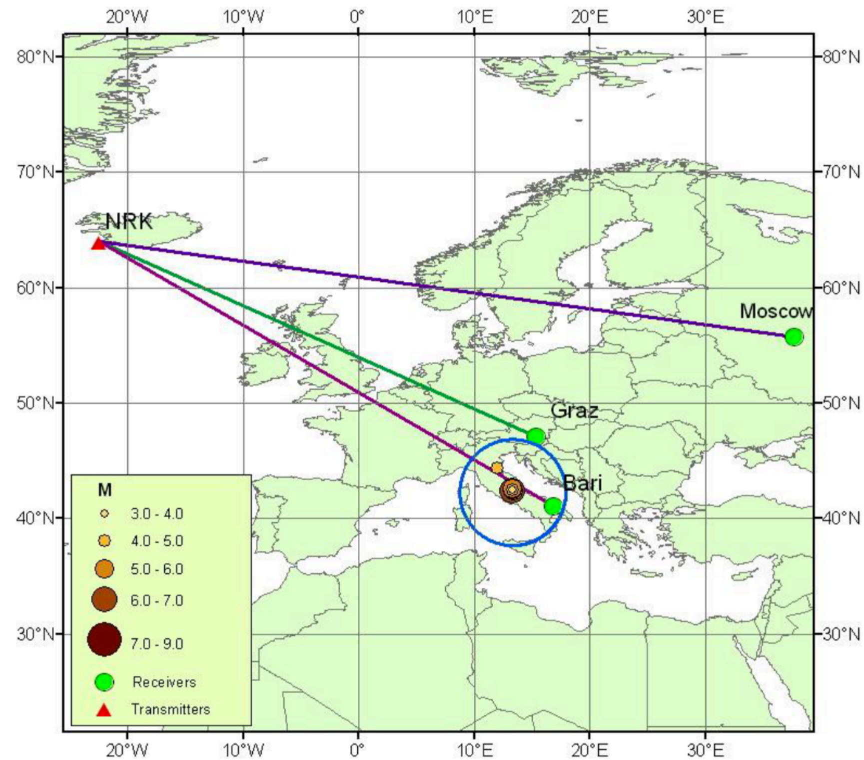

Map showing the NRK transmitter and the Moscow, Graz and Bari receivers. The seismic path is for the reception in Bari, while the other ones are control paths.

A. Rozhnoi, M. Solovieva, O. Molchanov, K. Schwingenschuh, M. Boudjada, P. F. Biagi, T. Maggipinto, L. Castellana, A. Ermini, and M. Hayakawa, Nat. Hazards Earth Syst. Sci., 9, 1727–1732, 2009

EARTHQUAKE IN L'AQUILA (ITALY) M=6,3, 6 APRIL 2009

Results in Moscow station.

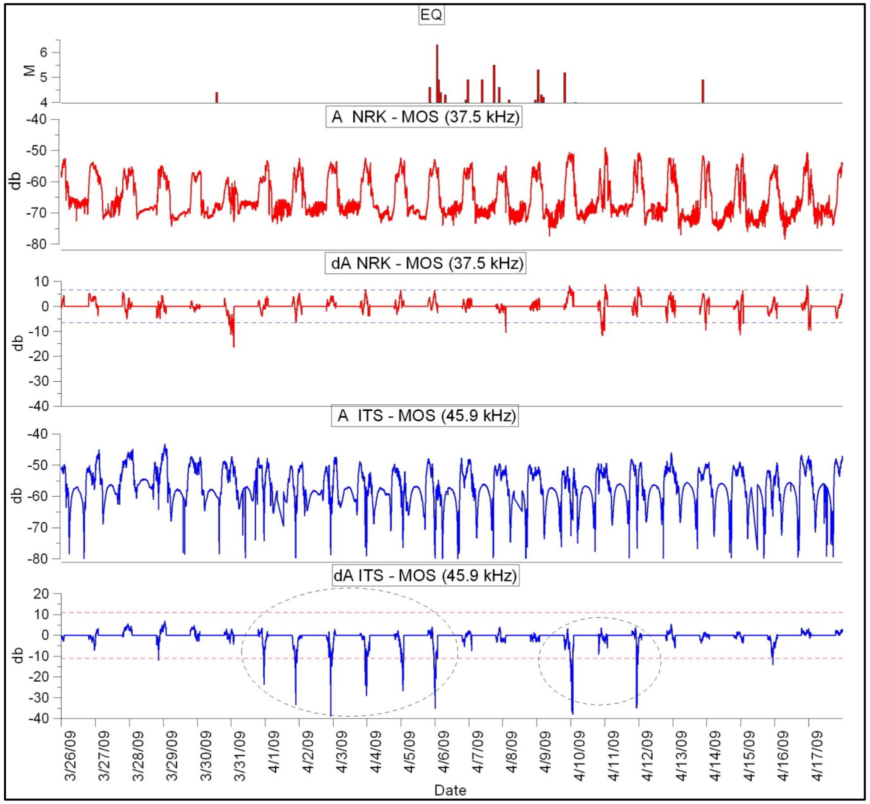

In the upper panel the magnitude of the main Abruzzo earthquakes from March 26 to April 17, 2009 is indicated. In the next panels, the signal amplitude (A) and the nighttime residual amplitude (dA) for the path NRK–MOS and ITS–MOS is reported. In the bottom panel the dashed ellipses indicate deviations of the real data from the averaged ones exceeding the 2σ (σ is the standard deviation) level, that is depicted by horizontal dotted line.

EARTHQUAKE IN L'AQUILA (ITALY) M=6,3, 6 APRIL 2009

Results in Graz station.

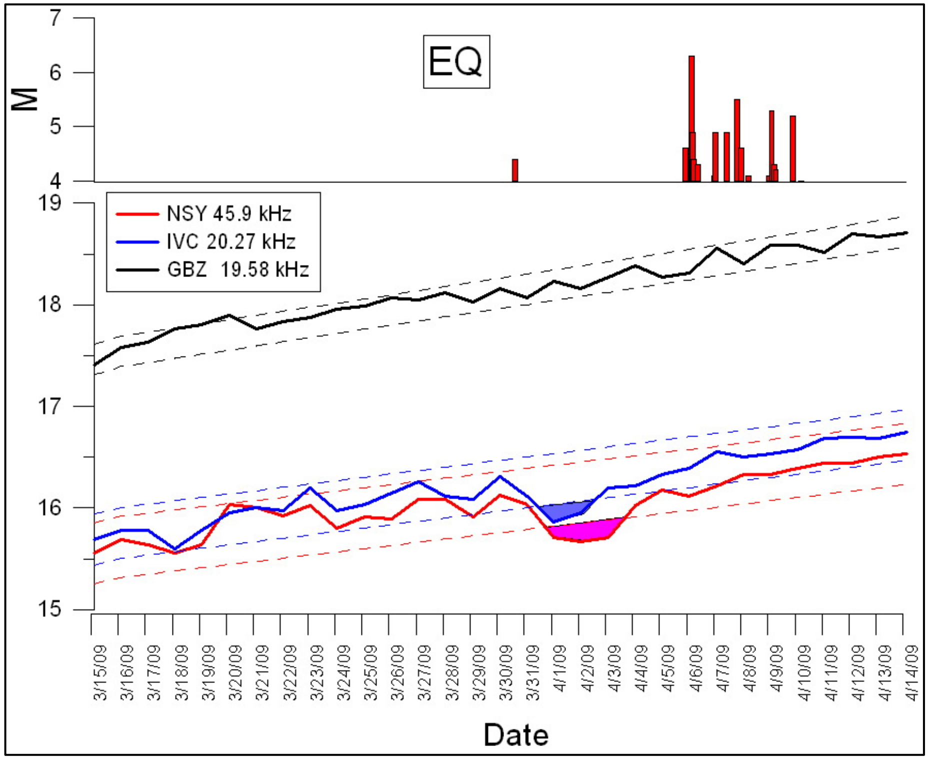

Sunset terminator times for GBZ (control path, black line), IVC (seismic path, blue line) and NSY (seismic path, red line) signals, in the period March 15 –April 14. The vertical axis indicates the time in hours from the midnight. The variation ranges of the terminator times related to undisturbed situations in the three cases are indicated by dash lines. The color fill zones indicate anomalies.

EARTHQUAKE IN L'AQUILA (ITALY) M=6,3, 6 APRIL 2009

Results in Bari station.

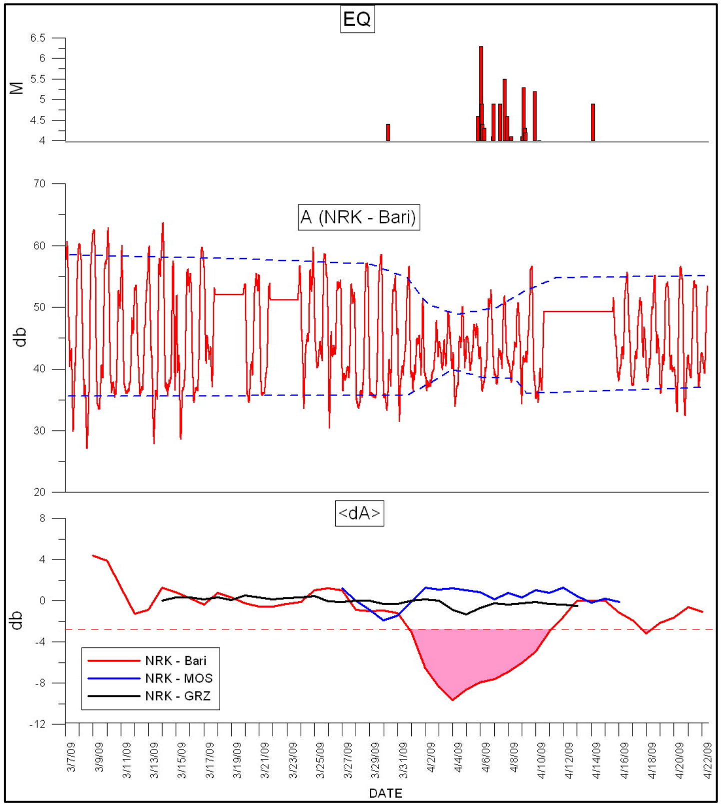

In the upper panel the magnitude of the main earthquakes from March 26 to April 17, 2009 is indicated. In the next panel, the signal amplitude (A) of the NRK signal recorded in Bari in the period March 7-April 22, 2009. In the last panel the nighttime residual amplitude (dA) for the path NRK-Bari, NRK-MOS and NRK-GRZ are reported. The color fill zone indicates values exceeding the 2σ level, represented by a horizontal dotted line, for the NRK-Bari path.

Results :

1. The anomalies revealed in VLF radio signals were detected in these signals prior the occurrence of the Abruzzo earthquake.
2. Their clear connection with the event was shown.
3. The obtained results confirm that the VLF radio signal method is a reliable and an efficient tool for the revelation of precursory activity on the occasion of large earthquakes.
4. It must be underlined that the observations of a multi-station VLF radio signals were considered

Ionospheric perturbations related to the earthquake in Vrancea area on November 22, 2014, as detected by electromagnetic VLF/LF frequency signals

Data from the European network of very low/ low frequency (VLF/LF) receivers has been used to study the response of the lower ionosphere to the earthquake of magnitude 5.5 in Vrancea area on November 22, 2014. Negative amplitude anomalies have been observed during 3 days before the earthquake and two days after, on the LF (45.9 kHz) signal passed above the seismic area. No perturbations have been found for the same signal in control paths during this period. Other possible influences both from above and below which can produce perturbations in the ionosphere have been taken into consideration.

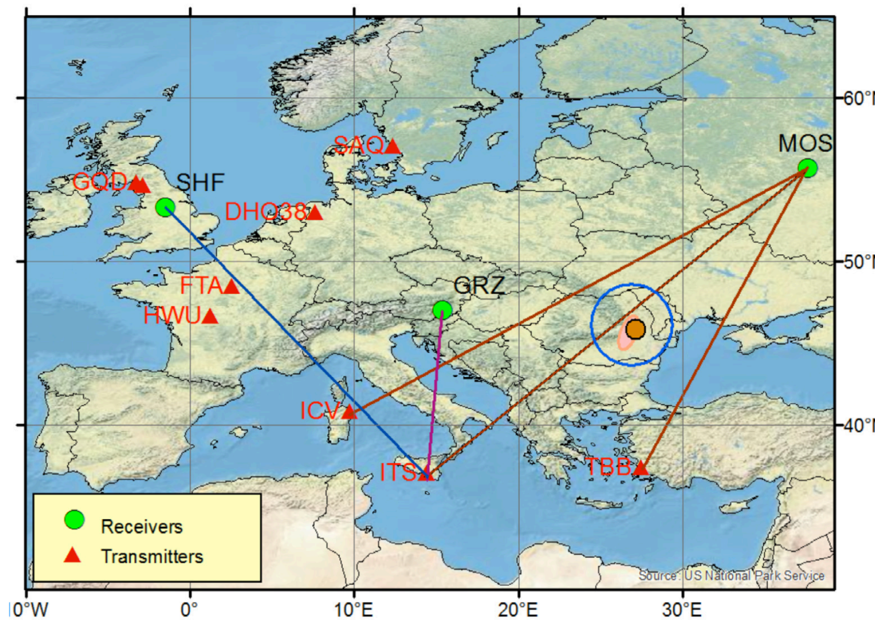

A map of the wave paths under analysis of the European network of VLF/LF stations. The position of the UltraMSK receivers in Moscow (MOS), Sheffield (SHF) and Graz (GRZ) and several transmitters in Europe is shown. Signals from three transmitters are analyzed in the work: ITS (45.9 kHz), ICV (20.27 kHz) and TBB (26.7 kHz). Pink ellipse shows the Vrancea zone in which the strongest earthquakes occur. Solid brown circle shows the epicenter of earthquake on November 22, 2014, with M=5.5 (USGS/NEIC). The area where possible precursors of an earthquake can be found is shown by the hollow blue circle.

The possible influences both from above (geomagnetic activity, proton bursts and relativistic electron fluxes) and below (cyclonic activity) which can produce perturbations in the ionosphere were taken into consideration. The recent development of the VLF observation systems in Europe, Asia, the Far East and US can provide useful information on the properties and position of the perturbation region in connection with seismic activity. The use of a network of observations makes it possible to separate the local VLF/LF perturbations from large-scale or global anomalies related to atmospheric circulation and space weather conditions. By utilising multi-station observations it is possible to determine the area of an impending earthquake.

M. Solovieva, A. Rozhnoi V. Fedun,
K. Schwingenschuh, M. Hayakawa, AnnGeophys, 58, 5, 2015,

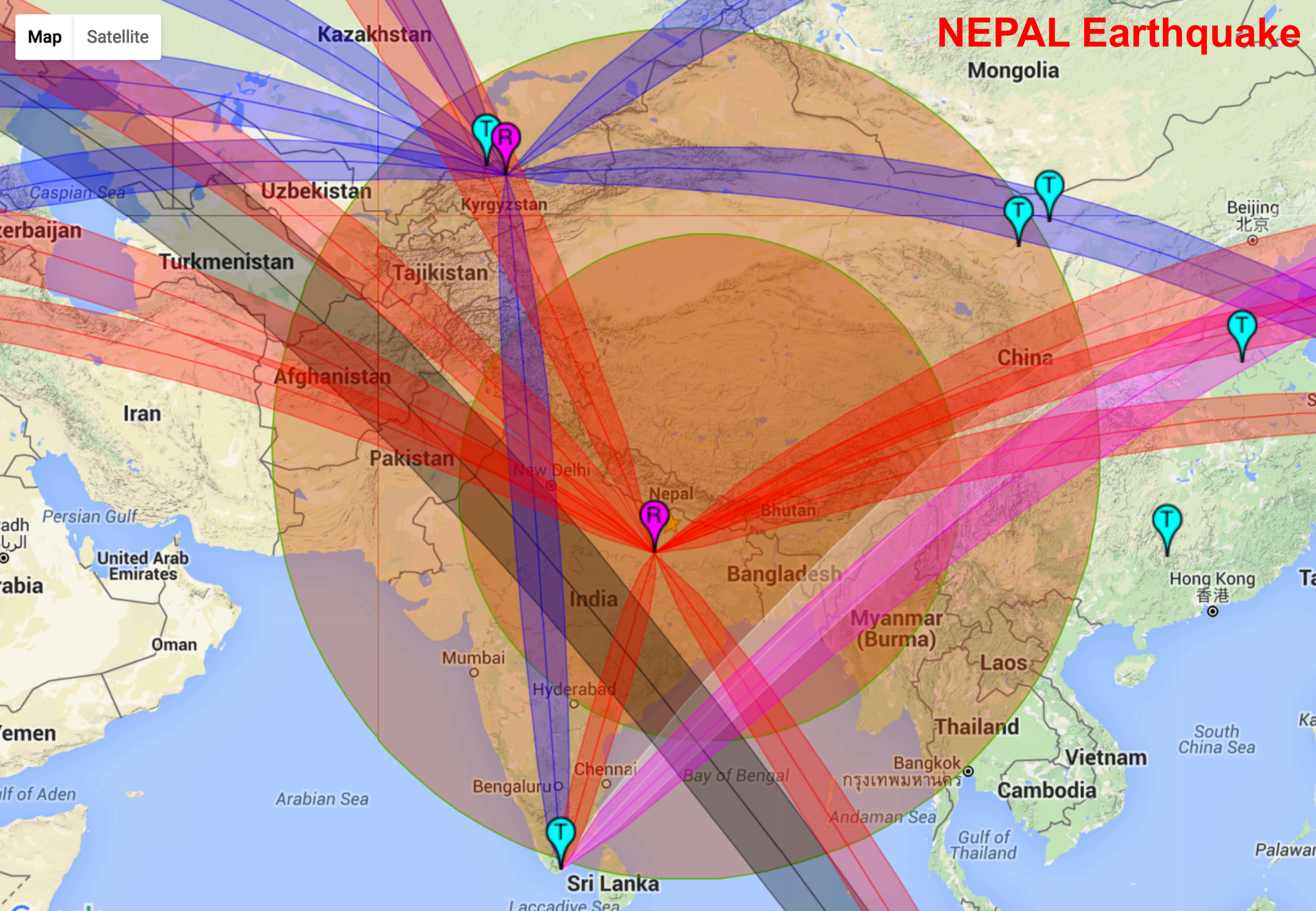
NEPAL Earthquake
Map
Satellite
Kazakhstan
Mongolia
Caspian Sea
Uzbekistan
Kyrgyzstan
Beijing
北京
Turkmenistan
Tajikistan
China
Afghanistan
Iran
Pakistan
New Delhi
Nepal
Bhutan
Persian Gulf
United Arab Emirates
Bangladesh
Hong Kong
香港
India
Myanmar (Burma)
Oman
Mumbai
Laos
Hyderabad
Thailand
South China Sea
Vietnam
Chennai
Bay of Bengal
Bangkok
กรุงเทพมหานคร
Bengaluru
Cambodia
Arabian Sea
Andaman Sea
Gulf of Thailand
Sri Lanka
Laccadive Sea

NEPAL Earthquake

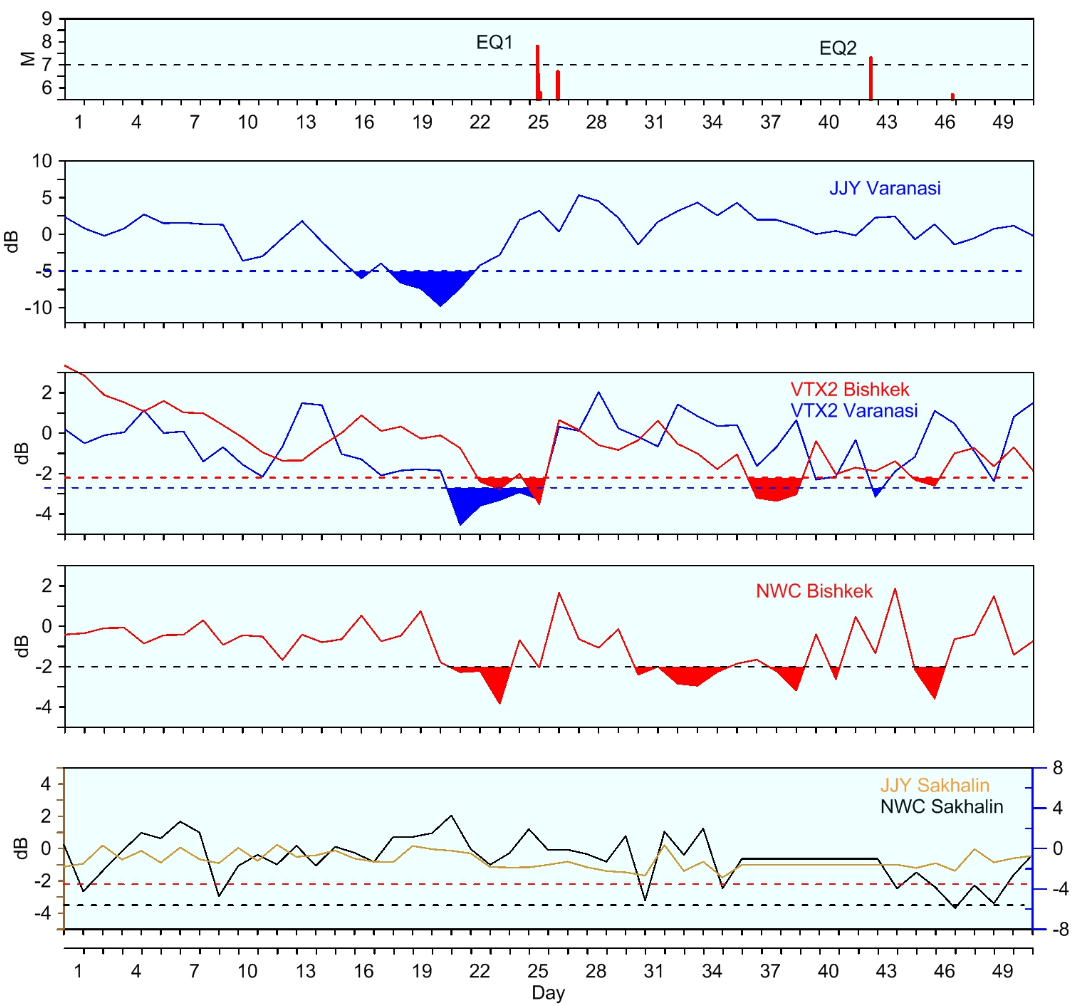

NEPAL Earthquake

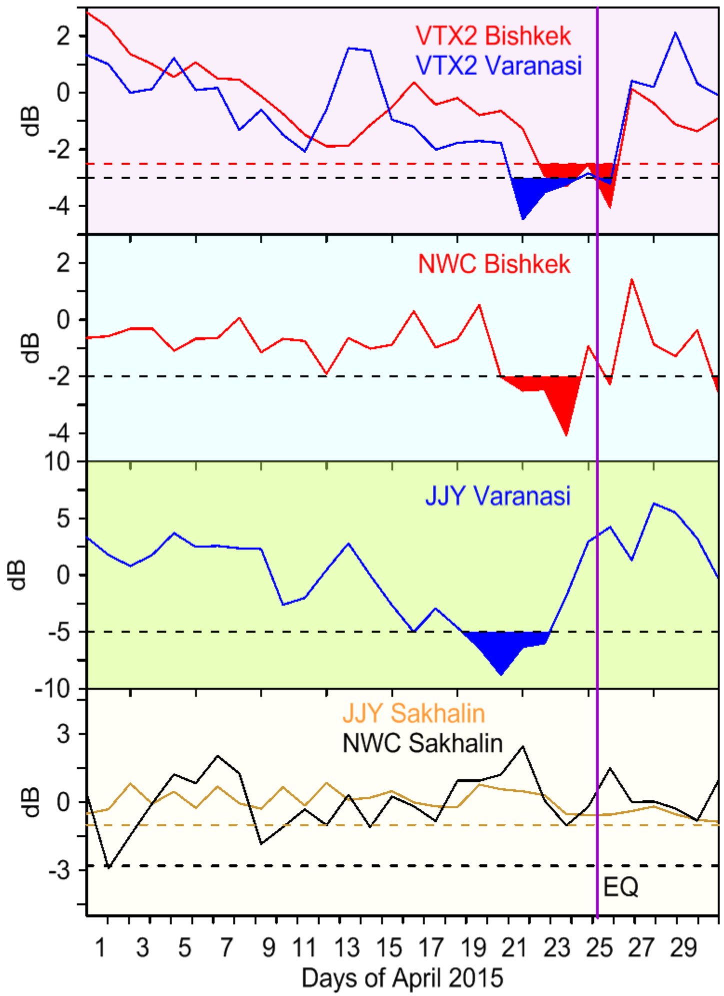

The results of analysis. The average residual amplitudes of the VLF/LF signals in nighttime are shown (top to down) for: VTX (17.0 kHz) transmitter recorded in Bishkek (red) and Varanasi (blue), NWC (19.8 kHz) transmitter recorded in Bishkek, JJY (40 kHz) transmitter recorded in Varanasi. The bottom panel shows JJY (yellow) and NWC (black) transmitter signals recorded in Yuzhno-Sakhalinsk stations (control 'aseismic' paths). The violet vertical line shows the occurrence time of the earthquake on 25 April, 2015. The color filled zones indicate values exceeding the 2σ (σ is the standard deviation) level, indicated by the horizontal dotted lines.

CURRENT DEVELOPMENT

- developing an online system which will collect and analyse in an automated regime the measured VLF/LF signals from redistributed VLF/LF receivers (currently eight + three) to obtain prediction of the occurrence of dangerous natural hazards;
- exploitation of simultaneous observations of various solar/magnetospheric processes by space-based instruments and ground-based VLF/LF receivers to investigate the coupling mechanisms between solar-magnetosphere events and the ionosphere-atmosphere response.